Modulated differential scanning calorimetry: Non-isothermal cure, vitrification, and devitrification of thermosetting systems

G. Van Assche, A. Van Hemelrijck, H. Rahier, B. Van Mele *

Department of Physical Chemistry and Polymer Science, Vrije Universiteit Brussel, Pleinlaan 2, 1050 Brussels, Belgium

Abstract

Vitrification of a reacting thermosetting system occurs when its glass transition temperature, T_g, rises to the reaction temperature, T. This phenomenon is not restricted to isothermal conditions only: for highly reactive systems, or when the applied heating rate is sufficiently small, vitrification occurs in non-isothermal conditions too. The reaction proceeds in mobility-restricted conditions. Devitrification is observed when the reaction temperature again surpasses T_g of the vitrified resin.

The non-isothermal vitrification and devitrification of two epoxy thermosetting systems have been studied using modulated differential scanning calorimetry (MDSC). A normalized mobility factor, which is directly based on the experimental heat capacity evolution, is proposed. For both organic resins, it is shown that the points for which this mobility factor equals 0.5 can be used to quantify the temperatures of vitrification and devitrification.

The mobility factor derived from heat capacity is compared to a normalized diffusion factor calculated from heat flow using chemical kinetics modelling. For the epoxy resins studied, both factors coincide. Therefore, the mobility factor can be used as a direct measurement of the change in the rate of reaction when T_g of the reacting system approaches T.

Isothermal and non-isothermal MDSC experiments enable the reaction mechanism, the vitrification and devitrification process, and models for diffusion control to be studied, and improved processing conditions for the cure of thermosetting resins to be developed.

Keywords: Devitrification; Diffusion control; Modulated differential scanning calorimetry; Thermosetting polymer; Vitrification

---

* Corresponding author. Tel. + 32-(0)2-629.32.76; fax, + 32-(0)2-629.32.78; e-mail, bvmele@vnet3.vub.ac.be

1. Introduction

In an earlier article [1], the benefits of Modulated Differential Scanning Calorimetry (MDSC) for studying thermosetting systems in isothermal conditions were reported. This renovating thermal analysis technique allows for simultaneous study of the chemical kinetics and vitrification of reacting polymers. Vitrification of a thermosetting system occurs when its glass transition temperature, T_g, rises to the reaction temperature, T. In this case, the material transforms from a liquid or rubbery state to a glassy state. For organic systems, the reduction in segmental mobility leads to a marked decrease in the rate of reaction, as the reaction becomes diffusion or mobility controlled [1–3].

In order to describe the decrease in the rate of reaction at vitrification, a mobility factor, DF^*, was proposed, based upon a normalization of the experimental heat capacity change. For the organic systems studied, this mobility factor coincides with a normalized diffusion factor, DF, which is calculated from the heat flow using chemical kinetics modelling [1].

Vitrification can occur in non-isothermal conditions as well [4, 5]. This fact can easily be disregarded, leading to misinterpretations concerning kinetics and glass transition behaviour. In this publication, MDSC results for the non-isothermal cure of two epoxy systems are presented.

1.1. (De)vitrification in non-isothermal conditions

In a non-isothermal experiment, T_g can rise up to the reaction temperature if the rate of increase in T_g (due to reaction) is higher than the heating rate. Thus, factors favouring the occurrence of vitrification in non-isothermal conditions are: low heating rates, highly reactive systems, and an important variation in T_g with reaction conversion, x. Upon vitrification, the rate of reaction decreases due to the onset of mobility restrictions. In the glassy state, the reaction continues at a lower rate. While the temperature further increases at a constant heating rate, the conversion nears completion and T_g nears the glass transition temperature of the fully cured network, $T_{g\infty}$. So, the rate of reaction, and also the rate of increase in T_g, will drop further, allowing the reaction temperature to surpass T_g again. This non-isothermal transformation of the glassy state to a liquid or rubbery state, called devitrification, is a phenomenon that does not occur in isothermal experiments. It is comparable with the glass transition observed upon heating a partially reacted (or unreacted) thermosetting system.

1.2. (De)vitrification and rate of reaction

As for isothermal experiments [1–3], a normalized diffusion factor, DF, can be derived from the heat flow using chemical kinetics modelling. This diffusion factor accounts for the lower rate of reaction in the vitrified state, $(dx/dt)_{obs}$, as compared to the chemical rate (in the absence of mobility control), $(dx/dt)_{kin}$, for the same temperature and conversion [1–3]

$$\left(\frac{dx}{dt}(x,T)\right)_{obs} = \left(\frac{dx}{dt}(x,T)\right)_{kin} DF(x,T) \qquad (1)$$

The diffusion factor DF ranges from unity in the unrestricted state, to zero in the frozen glass (for more details see Ref. [1]). To derive the diffusion factor from the observed heat flow, the kinetics for the chemically controlled reaction need to be well known, especially when studying non-isothermal reactions, since the temperature range covered by the non-isothermal reaction exotherm is usually much bigger than the range covered by multiple isothermal experiments.

The chemical rate of reaction can be modelled by the semi-empirical autocatalytic rate equation

$$\frac{\mathrm{d}x}{\mathrm{d}t} = (k_1 + k_2 x^m)(1 - x)^n \tag{2}$$

with k_1 and k_2 rate constants and m and n reaction orders [6]. Using rate constants obeying an Arrhenius law, the equation can be used for modelling both isothermal and non-isothermal experiments.

1.3. (De)vitrification and heat capacity

Literature results for vitrification and, especially, devitrification in non-isothermal experiments using torsional braid analyses [4, 5] and dielectric thermal analyses [7, 8], are scarce. Moreover, as indicated for isothermal experiments [1], these techniques give no quantitative information about the evolution of conversion or the rate of conversion with time and temperature.

In conventional DSC, non-isothermal vitrification can, in principle, be observed as a strong decrease in the rate of reaction. Due to the low heating rates required for most organic systems, the heat flow in diffusion-controlled conditions is often very small (see Section 3.1). This explains why it mostly stays unnoticed. Even if the drop in heat flow and its remaining small value is differentiated from baseline effects and thus not neglected, it is still impossible, firstly, to determine from a single DSC experiment whether this phenomenon is due to vitrification or to complex reaction kinetics, and secondly, to quantify it properly. However, it should be noted that during this diffusion-controlled cure, conversion and T_g sometimes rise substantially (see Section 3.1).

In a single, non-isothermal MDSC experiment, the evolution of the rate of reaction can be followed quantitatively in the non-reversing heat flow signal, while vitrification and also devitrification can be observed separately in the heat capacity signal. Thus, this technique allows for a more straightforward and quantitative interpretation.

The degree of (de)vitrification can be quantified using the normalized mobility factor, DF^*, based on the heat capacity variation, which is defined for isothermal conditions in Ref. [1] and which is rewritten here for non-isothermal conditions

$$DF^*(x,T) = \frac{C_p(x,T) - C_{pg}(x,T)}{C_{pl}(x,T) - C_{pg}(x,T)} \tag{3}$$

This equation states that variations in heat capacity C_p are normalized between unity for the liquid or unrestricted state (with heat capacity C_{pl}), and zero for a frozen

glassy state (with heat capacity C_{pg}) [1]. For quantitative results, the influence of both temperature and conversion on the reference states, C_{pl} and C_{pg}, needs to be taken into account. The conversion is a function of time and temperature, and can be determined by integration of the heat flow signal.

2. Experimental

A bifunctional epoxy (LY 556) cured with an anhydride hardener (HY 917) using an accelerator (DY 070), and a tetrafunctional epoxy (MY 720) cured with an amine hardener (HY 2954) were studied. All components are from Ciba-Geigy. These epoxy systems are the same as in Ref. [1]. All details concerning the raw materials and their processing, as well as a description of the instrumentation, the experimental procedure and the calculations are given in Ref. [1].

Modulated non-isothermal experiments on a TA instruments 2920 DSC with MDSC^{TM} option were performed at a rate of $0.2°C\,min^{-1}$, with a modulation amplitude of $0.10°C$ or $0.15°C$ and a 60 s period. When appropriate, a second heating of the fully reacted sample was made, under the same conditions, to determine the evolution of the heat capacity of the fully cured network. For partial cure reactions, the experiment was halted at a predetermined temperature. The glass transition temperature, T_g, and the residual cure were measured in a second heating from $-50°C$ to $275°C$ at $2.5°C\,min^{-1}$ with a $0.3°C$ per 60 s modulation. Note that not all experiments were performed using "heating only" conditions. However, this is not necessary for a correct interpretation of the results.

For kinetic modelling, experiments at multiple isothermal temperatures, ranging from $60°C$ to $120°C$, and at multiple scan rates, ranging from $2.5°C\,min^{-1}$ to $15°C\,min^{-1}$, were performed.

The temperatures $T_{1/2\Delta C_p}$ are the temperatures for which C_p is the mean of the heat capacities of the glassy and the liquid state, C_{pl} and C_{pg}, for the same temperature and conversion, i.e. the temperatures for which DF^* equals 0.5. More details concerning the calculation of DF^* are given below.

3. Results and discussion

3.1. Non-isothermal (de)vitrification

Fig. 1. shows the non-reversing heat flow and heat capacity as a function of temperature for the cure of the epoxy-anhydride at a rate of $0.2°C\,min^{-1}$. The heat capacity evolution for the completely cured resin, measured using identical conditions, is also shown. As for isothermal experiments, the non-reversing heat flow agrees well with the heat flow obtained in a conventional DSC experiment performed under the same conditions, with the exception of the modulation. The reaction exotherm shows a maximum at around $90°C$, followed by a decrease and a shoulder of more or less constant heat flow. The shoulder's height is 7% of the peak height or approx. $50\,\mu W$,
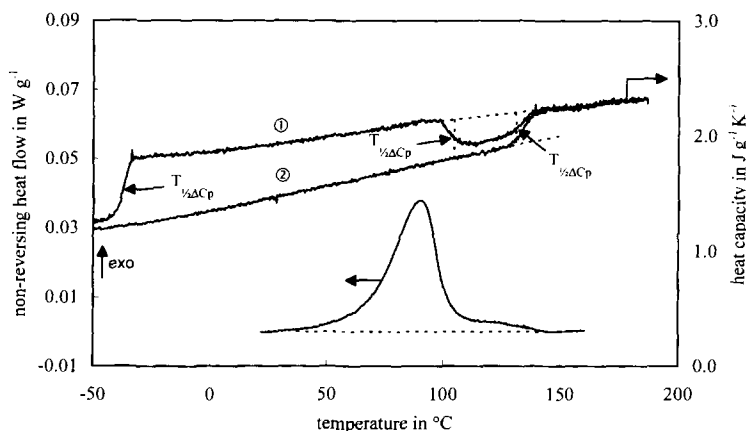
Fig. 1. Non-reversing heat flow and heat capacity for the non-isothermal cure of the epoxy–anhydride and heat capacity for the fully cured material, at 0.2°C min^{-1} with a 0.15°C per 60 s modulation. $T_{1/2\Delta C_p}$ is the temperature at half of the step in heat capacity.

and it spans a temperature interval of 40°C. In the heat capacity curve of the first heating, three transitions are observed. T_{go} of the uncured resin equals -37°C, with a $\Delta C_p(T_{go})$ of 0.49 J g^{-1} K^{-1}. The second transition, a decrease in C_p of 0.25 J g^{-1} K^{-1}, occurs at the instant the heat flow decreases. Near the end of the heat flow shoulder, C_p increases again with a ΔC_p of 0.20 J g^{-1} K^{-1}. In between the transitions, C_p rises slowly with temperature. In a second heating, $T_{g\infty}$ of the fully cured network amounts to 135°C, with a ΔC_p of 0.28 J g^{-1} K^{-1}. Measured against this second heating reference line, the temperatures at half of the heat capacity difference, $T_{1/2\Delta C_p}$, equal -37°C (T_{go}), 104°C and 131°C, respectively.

Using the experimental conditions of Fig. 1, the evolution of T_g with reaction temperature was determined from a residual cure of a number of partially reacted samples. Fig. 2a shows the heat capacity evolution for a partial cure reaction and the subsequent residual cure experiment. The first heating, at 0.2°C min^{-1}, was halted at a temperature of 103°C. The T_g observed in the second heating, at 2.5°C min^{-1}, equals 108°C. In Fig. 2b, the evolution determined from partial cure experiments is compared to T_g calculated using the conversion profile, obtained by numerical integration of the reaction exotherm of Fig. 1, and the T_g–x relation for the epoxy-anhydride system established earlier (see Fig. 12 in Ref.[1]). Below the dashed line for which T_g equals T, the material is in the liquid or rubbery state; above this line, the material is in the glassy state. Initially the material is in the glassy state, and devitrifiation occurs for a first time when T reaches T_{go}. The reaction starts at about 25°C. At first, T_g rises slowly, then more rapidly: at the heat flow maximum, T_g increases with a rate of 10°C °C^{-1}, or 50°C min^{-1}, which is much faster than the applied heating rate of 0.2°C min^{-1}. Vitrification occurs when T_g surpasses T at 101°C (T_{vit}). Due to vitrification, the rate of reaction quickly decreases. The rate of increase in T_g also drops and the T_g curve runs more or less parallel with T. A maximum difference $T_g - T$ of 7°C is reached. Then T_g
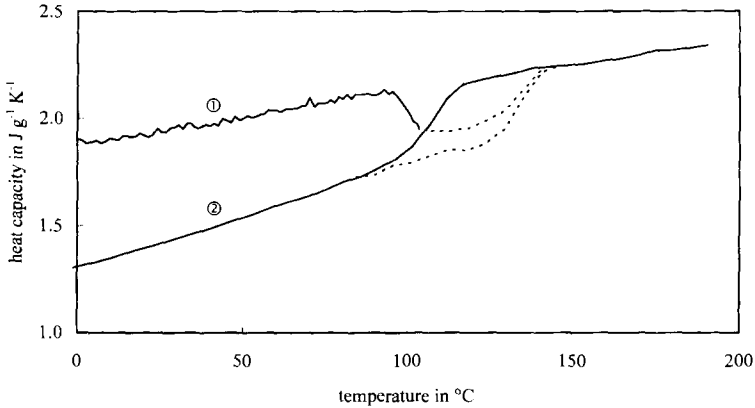
Fig. 2a. Evolution of the heat capacity for the first and second heating of a non-isothermal partial cure experiment of the epoxy–anhydride: first heating at 0.2°C min⁻¹ with a 0.15°C per 60 s modulation, halted at 103°C; second heating at 2.5°C min⁻¹ with a 0.3°C per 60 s modulation. The dotted line represents the evolution for full cure in the second heating (see Fig. 1).
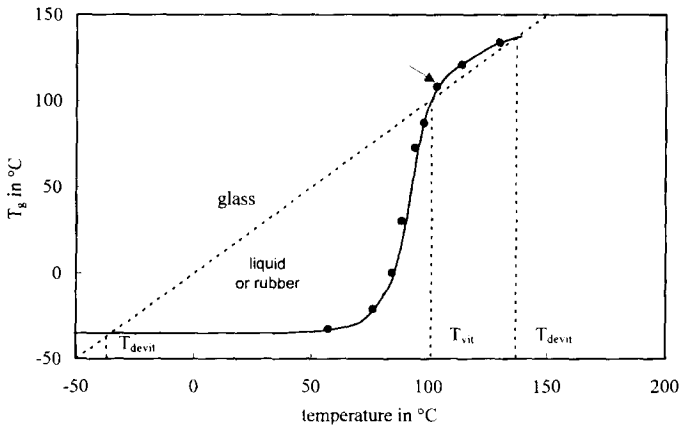
Fig. 2b. Evolution of the glass transition temperature, T_g, for the non-isothermal cure of the epoxy–anhydride at 0.2°C min⁻¹ with a 0.15°C per 60 s modulation: T_g(●) measured for partially reacted samples, and T_g calculated from the conversion out of the non-reversing heat flow signal of Fig. 1 and using the T_g–x relation [1] (solid line). The arrow indicates the experiment shown in a.

increases more slowly than T, and devitrification occurs at a temperature of 137°C (T_{devit}). Comparison of the evolutions of C_p and T_g (Figs. 1 and 2) shows that the three transitions in heat capacity, characterized by the temperatures $T_{1/2\Delta C_p}$, subsequently correspond to the devitrification, vitrification and devitrification processes. Therefore, the three $T_{1/2\Delta C_p}$ points obtained in a single non-isothermal modulated DSC experiment can be used to quantify vitrification and devitrification.

The results for the amine-cured epoxy for the same heating rate of $0.2°C \, min^{-1}$ are shown in Fig. 3. The overall picture is similar to the result for the epoxy–anhydride (Fig. 1). T_{g0} equals $-25°C$. The non-reversing heat flow passes through a maximum at 70°C, and then decreases sharply. Simultaneously, a sharp decrease in heat capacity occurs. The cure of another sample was stopped at this point. The glass transition temperature measured in the second heating is 81°C. Considering the reactivity of this resin, these data confirm the occurrence of vitrification at the instant that heat flow and heat capacity decrease in Fig. 3. Between 85°C and 235°C, a temperature interval of 150°C, a small heat flow is still observed (25–60 μW). A second (low) maximum is even attained around 200°C, then the heat flow decreases to reach the baseline level near 235°C. Over the 150°C–wide interval, C_p of the curing network (first heating) and C_p of the fully cured, vitrified resin (second heating) slowly converge. The first and second heating both show a small increase in C_p (0.1 J g^{-1} K^{-1}) ending at approx. 255°C. Since the reaction is completed near 235°C, this change in C_p corresponds most probably to devitrification. Neither this transition nor $T_{g\infty}$ can be determined unambiguously because the step change in heat capacity is small, and because degradation of the polymer network becomes prominent at 275°C. The smallness of $\Delta C_p(T_{g\infty})$ is due to the high crosslink density of the fully cured resin, so that less mobility will be freed beyond $T_{g\infty}$ due to the restrictions of the tight network. For the tetrafunctional epoxy–amine, the final crosslink density is higher than for the bifunctional epoxy–anhydride, causing a higher $T_{g\infty}$ (approx. 255°C) and a smaller $\Delta C_p(T_{g\infty})$.

Before vitrification of the epoxy–amine system, the heat capacity increases with reaction conversion, as deduced from the peak in heat capacity coinciding with the reaction exotherm (Fig. 3). For the epoxy–anhydride, the influence of reaction conversion is much smaller. During the reaction (before vitrification, or up to a conversion of
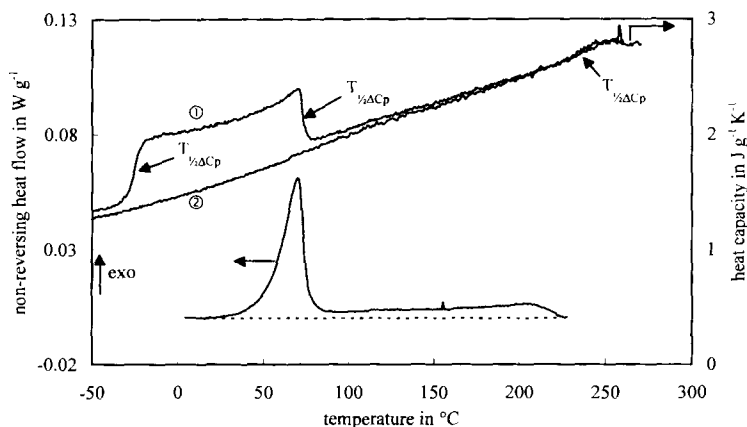
Fig. 3. Non-reversing heat flow and heat capacity for the non-isothermal cure of the epoxy–amine and heat capacity for the fully cured material, at $0.2°C \, min^{-1}$ with a 0.15°C per 60 s modulation. $T_{1/2\Delta C_p}$ is the temperature at half of the step in heat capacity.

84%), only a limited variation of C_p is observed (Fig. 1). This is consistent with the results for isothermal experiments: an important increase in C_p with conversion was seen for the amine-cured epoxy, whereas for the anhydride-cured epoxy a minor decrease in C_p was observed [1].

3.2. Chemical kinetics modelling

To calculate the non-isothermal heat flow diffusion factor, the rate of reaction in the absence of mobility restrictions has to be known. To this end, multiple isothermal and non-isothermal MDSC experiments, for different temperatures and heating rates, are performed. For each experiment, a set of datapoints in the region *before* vitrification are withheld (this criterion can be checked easily by examining the heat capacity evolution). The autocatalytic rate equation (Eq. (2)) is numerically integrated, and the parameters are fitted simultaneously for all experimental rate of conversion versus time profiles, both isothermal and non-isothermal. Note that measured temperature–time profiles are used, to allow for the small deviations between sample and program temperature in a heat flux DSC. The resulting set of four Arrhenius parameters and two reaction orders of Eq. (2) can be used to calculate the evolution of conversion and rate of conversion in the absence of mobility restrictions, for all temperature profiles.

Figures 4a–c show some of the experimental and optimized rate of conversion profiles for the epoxy–anhydride system. The agreement between experiment and model is very satisfactory, considering the wide range of experimental conditions depicted (notice that all optimized profiles result from one and the same optimized parameter set, so that small deviations between experiment and model in some profiles are due to this optimization strategy). In the isothermal experiments, the experimental
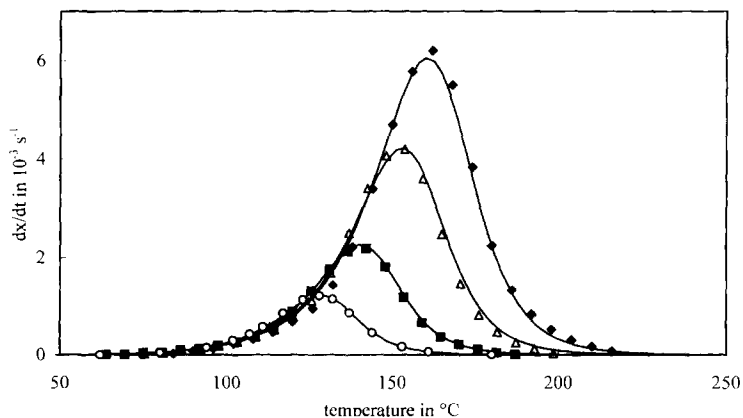
Fig. 4a. Rate of conversion versus reaction temperature for the non-isothermal cure of the epoxy–anhydride. MDSC experimental points for 2.5 (○), 5 (■), 10 (△), 15°C min^{-1} (◆), and optimized profiles for chemical control (solid line).
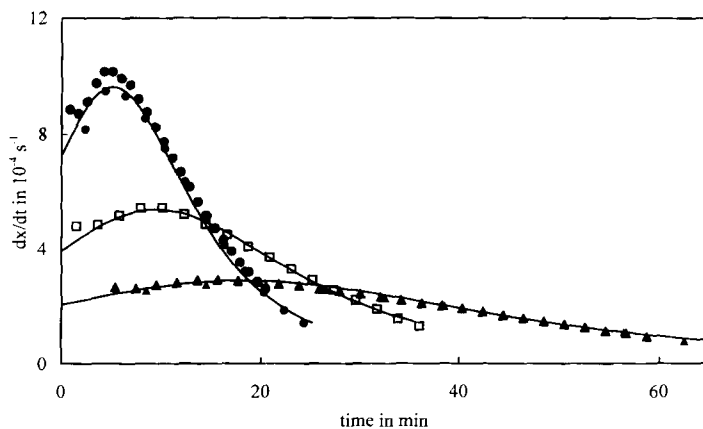
Fig. 4b. Rate of conversion versus reaction time for the isothermal cure of the epoxy–anhydride. MDSC experimental points for 100 (▲), 110 (□), and 120°C (●), and optimized profiles for chemical control *before* vitrification (solid line). The experiment at 120°C was performed twice, illustrating the reproducibility of the results.
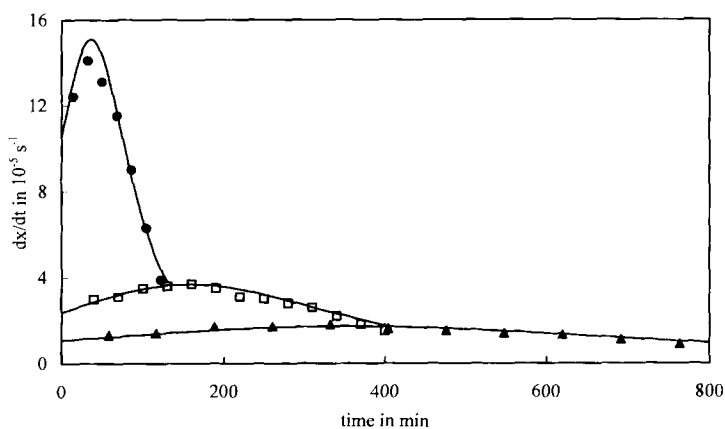
Fig. 4c. Rate of conversion versus reaction time for the isothermal cure of the epoxy–anhydride. MDSC experimental points for 60 (▲), 70 (□) and 90°C (●), and optimized profiles for chemical control *before* vitrification (solid line).

rate is not taken into account after vitrification. For the non-isothermal experiments shown, vitrification is not observed.

Because of a different composition and reactivity, the amine-cured epoxy needs to be modelled separately, resulting in a second set of parameters. For this system, an equivalent, quantitative description of the chemically controlled kinetics is obtained.

3.3. Determination of diffusion and mobility factor

Fig. 5a compares the experimental conversion for the cure of the epoxy–anhydride at $0.2°C$ min^{-1} with the conversion obtained by numerical integration of the chemical rate equation for the same temperature profile. Up to vitrification, both curves nearly coincide. After vitrification, the experimental conversion increases more slowly than in the absence of mobility restrictions. Unity is reached after devitrification. In order to calculate the diffusion factor, DF, the observed rate of conversion, $(dx/dt)_{obs}$, has to be compared to the chemical rate, $(dx/dt)_{kin}$, for the same conversion and temperature (Eq. (1)). The evolution of both rates is given in Fig. 5b. Notice that the chemical rate plotted is not the derivative versus time of the calculated conversion profile given in Fig. 5a. For each temperature, $(dx/dt)_{kin}$ is calculated using the kinetic model (Eq. (2)) and the experimental conversion corresponding to that temperature.

Similar results for the cure of the epoxy–amine at $0.2°C$ min^{-1} are given in Fig. 6a and b. Once more, the influence of vitrification is more clearly visible for this system. Vitrification occurs at $73°C$, corresponding to 56% conversion. Then the conversion increases more slowly, only reaching unity at $235°C$. Therefore, a high concentration of unreacted functional groups is still present at elevated reaction temperatures, e.g. a residual conversion of 20% at $160°C$. Thus, the driving force for chemical reaction becomes very big, which is equivalent to a very high $(dx/dt)_{kin}$ in Fig. 6b, with a maximum for a residual conversion of 15% at $180°C$.

The non-isothermal mobility factor, DF^*, is determined using the heat capacity. When considering the heat capacity evolution in Figs. 1 and 3, an important increase in heat capacity with rising temperature is observed. Moreover, the conversion also affects this evolution. This is deduced from the peak in heat capacity coinciding with the reaction exotherm (see Fig. 3), and from the observation that the heat capacity in the vitrified state at $-50°C$ decreases as conversion increases (compare the first and
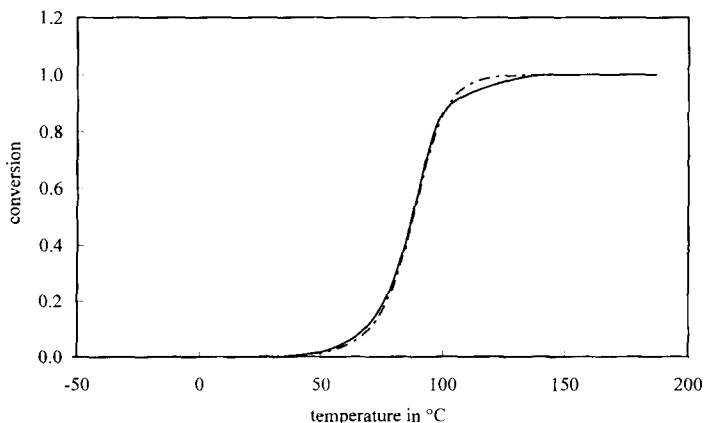
Fig. 5a. Conversion versus reaction temperature for the cure of the epoxy–anhydride at $0.2°C$ min^{-1}. Experimental profile (solid line) and profile calculated for chemical control (dot-dashed line).
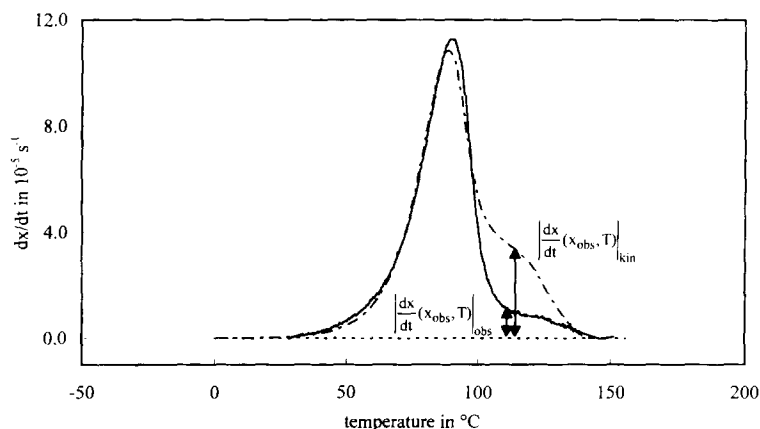
Fig. 5b. Rate of conversion versus reaction temperature for the cure of the epoxy– anhydride at 0.2°C min^{-1}. Experimental rate $(dx/dt)_{obs}$ (solid line) and rate expected for the same conversion and temperature in the absence of mobility restrictions, $(dx/dt)_{kin}$ (dot-dashed line).
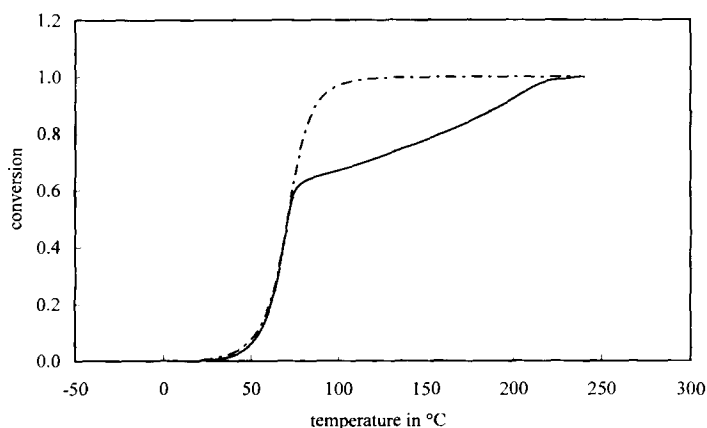
Fig. 6a. Conversion versus reaction temperature for the cure of the epoxy–amine at 0.2°C min^{-1}. Experimental profile (solid line) and profile calculated for chemical control (dot-dashed line).

second heating in Figs. 1 and 3). The curves for zero and full conversion are not simply shifted, since the influence of temperature is also different. This can be seen from the different evolution of C_p for the liquid or rubbery states before vitrification and after devitrification. However, DF^* should mirror the reduction of mobility due to vitrification, and not the changes in heat capacity due to the reaction itself. Therefore, the effects of both temperature and conversion should be incorporated in both C_{pl} and C_{pg} (Eq. (3)). To this end, the evolutions with temperature of C_{pl} and C_{pg} were
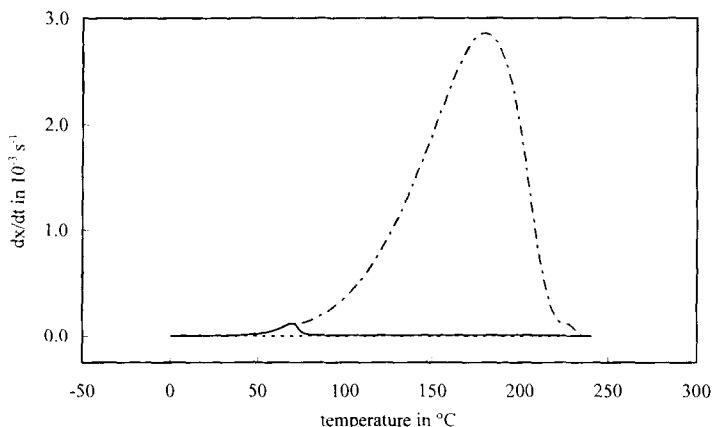
Fig. 6b. Rate of conversion versus reaction temperature for the cure of the epoxy–amine at 0.2°C min^{-1}. Experimental rate $(dx/dt)_{obs}$ (solid line) and rate expected for the same conversion and temperature in the absence of mobility restrictions, $(dx/dt)_{kin}$ (dot-dashed line).

determined for zero and full conversion. Subsequently, the evolution with conversion was assumed to be linear. This assumption is supported by a linear variation of C_p with conversion in isothermal measurements [1]. The resulting evolutions of $C_{pl}(T,x)$ and $C_{pg}(T,x)$ are shown in Fig. 7. An equivalent approach was used for the epoxy-amine system.
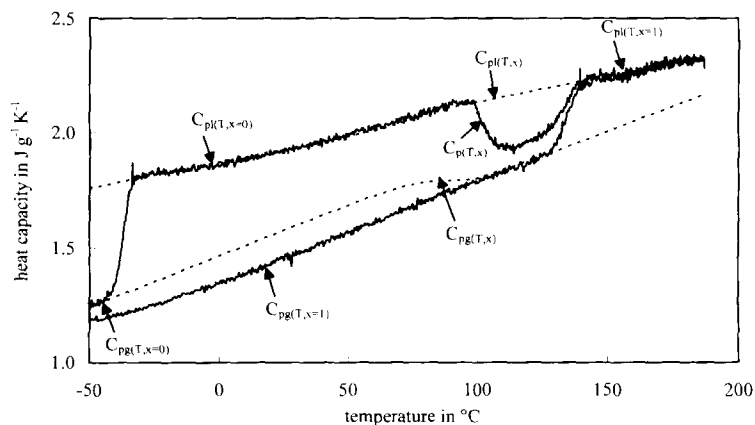
Fig. 7. Experimental heat capacity profiles (solid line) versus reaction temperature for the first (cure) and second heating of the epoxy–anhydride at 0.2°C min^{-1}. Calculated reference profiles for the heat capacity of the liquid or rubbery state, C_{pl}, and the glassy state, C_{pg} (dashed lines).

The non-isothermal diffusion and mobility factors, deduced from heat flow and heat capacity as outlined in Sections 1.2 and 1.3, are given in Figs. 8 and 9 for the anhydride- and amine-cured epoxy, respectively.

The diffusion factor, DF, can only be determined when the heat flow due to reaction (or the rate of reaction) is sufficiently high. In the temperature range between vitrifica-
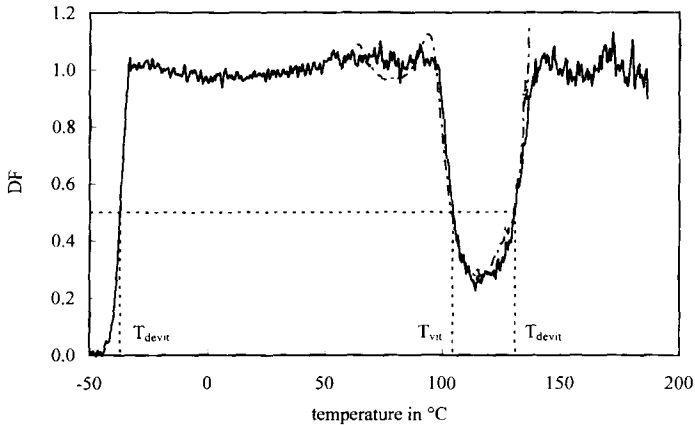
Fig. 8. Comparison of the mobility factor DF^* based on heat capacity (solid line) and the diffusion factor DF based on heat flow (dot-dashed line) for the cure of the epoxy–anhydride at 0.2C min^{-1}. T_{vit} and T_{devit} are respectively the temperatures at vitrification and devitrification ($DF^* = 0.5$).
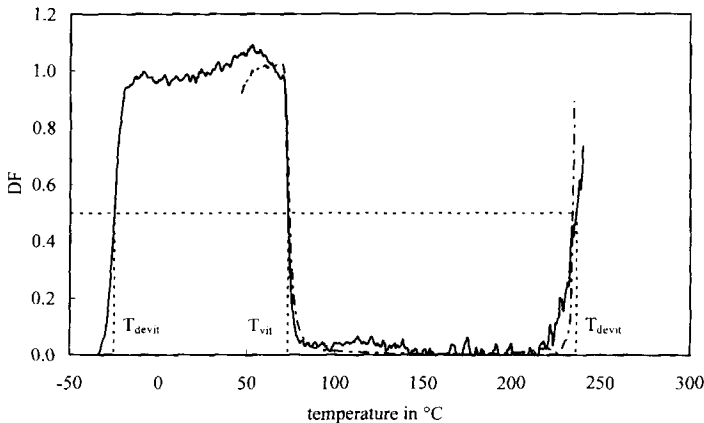
Fig. 9. Comparison of the mobility factor DF^* based on heat capacity (solid line) and the diffusion factor DF based on heat flow (dot-dashed line) for the cure of the epoxy–amine at 0.2°C min^{-1}. T_{vit} and T_{devit} are respectively the temperatures at vitrification and devitrification ($DF^* = 0.5$).

tion and devitrification, the agreement is very good. For the two resins, both factors give quantitatively the same results concerning the temperature and mode of decrease (vitrification) and increase (devitrification), as well as the level reached in between. Limited deviations of the heat flow diffusion factor are seen before vitrification and after devitrification. A first reason is that the kinetic model does not perfectly fit the observed rate of conversion profile, leading, for example, to values higher than unity for DF. One should bear in mind that the parameters are optimized for multiple experiments, which results in a model that is valid for a wide range of conditions, but also in a somewhat lesser fit for the individual experiments. A second source of error for DF is the small rate of conversion at the start and end of the reaction exotherm. When the heat flow is almost zero, small deviations lead to big errors in DF.

The mobility factor DF^* can be given for the entire temperature range, since it is calculated directly from the measured heat capacity and the reference lines C_{pl} and C_{pg}.

3.4. Comparison of diffusion and mobility factor of the epoxy thermosetting systems

As the diffusion factor and mobility factor coincide very well, the evolution of the normalized heat capacity gives a direct indication on diffusion-controlled cure, even in non-isothermal conditions.

For both thermosetting systems, the mobility factor shows the increase in mobility at T_{go}, followed by an interval of full mobility (DF^* equal to unity). At certain combinations of temperature and conversion, vitrification (T_{vit}) and devitrification (T_{devit}) occur at a value for DF^* equal to 0.5: the mobility factor first decreases (from 1 to below 0.5), to increase again to 1 at a higher temperature.

In addition to the transition temperatures, the curves give information concerning the extent of vitrification during the diffusion-controlled or mobility-restricted cure. For the anhydride-cured system the lowest level of DF^* is 0.25. This indicates that the material only partially vitrifies: 25% of mobility is still available at the minimum. In contrast, for the amine system, DF^* drops immediately to a level close to zero; the material almost completely vitrifies. T_g for the epoxy–amine increases more above the cure temperature than for the epoxy–anhydride. This increased difference between T_g and T corresponds to a higher degree of vitrification (with the condition that the width of the glass transition is more or less equal for both resins), which is in correspondence with the stronger decrease in mobility factor. The higher degree of vitrification for the epoxy–amine is in accordance with the results for the isothermal experiments, where the increase in the conversion after vitrification is higher for the epoxy–amine than for the epoxy–anhydride [1]. In a non-isothermal experiment, analogous behaviour can be expected. This different vitrification behaviour is related to the reactivity and chemical structure of the reagents, as explained in Ref. [1].

Considering the results of both organic systems, the impact of vitrification on the cure is much stronger for the epoxy–amine. For the same heating rate, vitrification occurs at a lower temperature and conversion for the epoxy–amine. This is due to a higher reactivity on the one hand, and to a faster increase of T_g with conversion on the other. For the amine system, the $T_{g\infty}$ of 255°C causes devitrification to occur at

a temperature approx. 150°C above vitrification. The importance of this extended mobility-restricted cure on the final material's properties should be emphasized. For this amine-cured tetrafunctional epoxy, an increase in T_g of approx. 150°C, corresponding with a residual cure of approx. 40% and a reaction enthalpy of more than 200 J g^{-1}, is caused by diffusion-controlled reactions and drastically influences the final network structure (crosslink density). An accurate quantitative description of this process is indispensable for an optimized thermoset processing.

Moreover, for the epoxy-amine system, a strong vitrification is still observed for experiments at heating rates of 10°C min^{-1} and higher [9]. This indicates that attention needs to be payed when using non-isothermal experiments to study the reaction kinetics: the reaction is not *de facto* occurring in chemically controlled conditions, even at higher heating rates. A more thorough discussion of the influence of the heating rate on the vitrification behaviour will be presented later [9].

4. Conclusions

The results obtained indicate that MDSC is a very useful technique for studying the vitrification behaviour in thermosetting systems. Using a single non-isothermal MDSC experiment, vitrification and devitrification can be observed as step changes in the heat capacity signal, while at the same time the evolution of the reaction rate is followed in the non-reversing heat flow signal. The additional information available in the heat capacity evolution is a key factor for the correct interpretation of the heat flow signal.

A mobility factor based on heat capacity, DF^*, is proposed in this work. For both epoxy resins studied, it was shown that all three points for which DF^* equals 0.5 can be used to quantify the temperatures of vitrification and devitrification. Moreover, the DF^* curve gives information on the degree of vitrification while the reaction occurs in mobility-restricted conditions.

As for isothermal experiments [1], the non-isothermal mobility factor presented in this paper coincides very well with the diffusion factor, calculated from the non-isothermal heat flow via chemical kinetics modelling, and describing the effects of diffusion control on the rate of conversion of the cure reaction.

Although the two resins behave quite differently, this coincidence between the non-isothermal mobility factor and diffusion factor is valid for both systems. Therefore, the mobility factor can be used for a quantitative description of their altered rate of conversion in the (partially) vitrified state: the decrease in rate during vitrification, the increase in rate during devitrification, and the diffusion-controlled rate in the (partially) vitrified region in between both processes.

Using the mobility factor proposed and the non-reversing heat flow of both isothermal and non-isothermal MDSC experiments, the effects of polymer structure and reaction mechanism on the partially vitrified cure reaction could be studied, theoretical models for diffusion control could be evaluated, and improved processing conditions for thermosetting resins could further be developed with Temperature–Time–Transformation (TTT) and Continuous-Heating–Transformation (CHT) diagrams [4, 5, 9].

Acknowledgements

References

[1] G. Van Assche, A. Van Hemelrijck, H. Rahier and B. Van Mele. Thermochim. Acta, 268 (1995) 121.
[2] G. Wisanrakkit and J.K. Gillham, J. Coat. Technol., 62 (1990) 35.
[3] H. Stutz, J. Mertes and K. Nuebecker, J. Polym. Sci. Part A: Polym. Chem., 31 (1993) 1879.
[4] G. Wisanrakkit and J.K. Gillham, J. Appl. Polym. Sci., 42 (1991) 2453.
[5] G. Wisanrakkit, J.K. Gillham and J.B. Enns, J. Appl. Polym. Sci., 41 (1990) 1895.
[6] M.R. Kamal, Polym. Eng. Sci., 14 (1974) 231.
[7] M.G. Parthun and G.P. Johari, Macromolecules, 25 (1992) 3149.
[8] K.A. Nass and J.C. Seferis, Polym. Eng. Sci., 29(5) (1989) 315.
[9] G. Van Assche, A. Van Hemelrijck, H. Rahier and B. Van Mele, to be published.